In: 10th International Conference on Advanced Robotics (ICAR 2001), Budapest, 22.-25. August 2001

Manipulating Deformable Linear Objects: Characteristics in Force Signals for Detecting Contact State Transitions

Antoine SCHLECHTER and Dominik HENRICH

Embedded Systems and Robotics Lab. (RESY)
Faculty of Informatics, Building 48
University of Kaiserslautern, D-67653 Kaiserslautern, Germany
E-Mail: [a_schlec, henrich]@informatik.uni-kl.de, http://resy.informatik.uni-kl.de/

Abstract

This paper deals with the handling of deformable linear objects (DLOs), such as hoses, wires or leaf springs. It investigates the a priori knowledge about the 6-dimensional force/torque signal for a changing contact situation between a DLO and a rigid polyhedral obstacle. The result is a complete list, containing for each contact change the most significant combination of force/torque signal components together with a description of the expected signal curve. This knowledge enables the reliable detection of changes in the DLO contact situation and with it the implementation of sensor-based manipulation skills for all possible contact changes.

Keywords: Non-rigid objects, Force/torque sensing, Manipulation skills, Assembly

1. Introduction

Manipulating deformable linear objects (DLOs), such as hoses, wires or leaf springs with an industrial robot system involves coping with many uncertainties. At the start of a manipulation process, it is hard to determine the exact shape of a DLO. The shape depends on the object's manipulation history and may vary for each individual DLO. In addition, the shape of the DLO changes due to the inevitable action of gravity and contact forces. Unfortunately, these variations are typically very difficult to predict with sufficient precision. In order to compensate for these uncertainties, an obvious approach is based on the use of sensors.

Kraus and McCarragher used a wrist-mounted force/torque sensor to insert a bending beam into a narrow slit [4]. Nakagaki et al. used a force/torque sensor and a vision system to insert a wire into a hole under friction [8]. This research investigates the solution of clearly specified single tasks, but it is not clear how these methods may be re-used in other, similar situations.

As far as rigid work pieces are concerned, much previous research addressed the problem of developing robust and flexible routines for typical assembly or disassembly tasks. The basic idea is to set up a library of encapsulated, sensor-based routines, which can be used as a construction kit to efficiently solve complex assembly problems. Hasegawa et al. presented the force-based skills move-to-touch, rotate-to-level and rotate-to-insert, and demonstrated their effectiveness for disassembling a small valve [2]. Morrow and Khosla used sensorimotor primitives to compose skills for insertion of various plug-in connectors [7].

According to Morris and Haynes [5], the performance of assembly tasks can be regarded as stepwise increasing the number of constraints for one of the mating parts by establishing contact with other parts. Detecting and manipulating the contact state of the mating parts is a key problem for developing manipulation routines. Any routine changing the contact state of the mating parts (like establishing point contact, transferring point contact to face contact, etc.) forms a module of the construction kit for assembly operations.[1]

Later research addressed the problem of finding a universal set of manipulation skills. Morrow and Khosla proposed a taxonomy to develop manipulation task primitives for composing sets of robot skills likely to cover a given domain [6].

Since this principle proved to be successful in the handling of rigid work pieces, the next step was to extend it to the handling of deformable objects. For this purpose, Henrich et al. introduced a set of contact states that enumerates all possible single contact situations between a DLO and a rigid convex polyhedron [3] and analyzed the possible transitions between these contact states [9]. This model describes a DLO as an edge E with the free endpoint as one vertex V. Convex polyhedrons consist of faces F, edges E and vertices V. Single contact states may then be described by the respective elementary parts in contact, e.g., V/F stands for a vertex face contact. In the following, we always denote the DLO contact part first. If a contact state remains unchanged during a small gripper movement we call it stable, otherwise we call it instable. *Direct* contact state transitions are given by a start-

[1] Those modules are called manipulation skills by other authors. However, the usage of this term is not uniform.

ing and an ending state (both stable), *indirect* transitions are given by a starting (stable), a temporary (instable), and an ending state (stable).

Our objective is the implementation of a complete library containing a macro-operation for each contact state transition. The basic approach is the realization of a knowledge-based sense of touch. For a given contact state transition, the force/torque signal during transition is predicted. If the expected signal is successfully detected within the real sensor data, the transition is recognized. Remde [10] followed this approach and performed an intuitive non-vector analysis of the force/torque signals for each transition.

In this paper, a more complete vector oriented study based on a mathematical model is performed. The study makes assumptions about robot motion directions and predicts force and motion directions, together with the expected signals, well suited for an algorithmic recognition process.

The rest of the paper is organized as follows: Section 2 describes the general method for force signal analysis used to detect transitions of contact states. The method is illustrated by two examples in Section 3 and Section 4. Then, Section 5 presents the complete list of characteristics for each transition. The conclusion includes a short evaluation based on a primitive detection algorithm.

2. Force signal analysis of contact state transitions

For easy detection of a given contact state transition, a clear change in the force signal at the transition point in time is needed. This can be a slope change or a discontinuity. Therefore, we assume that for the robot motion, the movement is parallel to the actual/new plane of contact or perpendicular to the new/actual plane of contact. These movements will result in a constant force before/after the transition or in a great force change, respectively. The plane of contact is defined as the contact face, or as the plane containing both the contact edge and the DLO tangent in the contact point.

Based on these assumptions, the force and torque during the transition are first analyzed in a theoretical model. The derived predicted force signals are verified by experiment. Then, a linear combination of the six dimensions of force and torque containing the most significant sensor information for transition detection is specified. Finally, the expected signal is described as a piecewise linear function: it is indicated whether there is a positive-, a negative- or no discontinuity at all (a); what the sign of the slope before (b) and after (c) the transition is; and whether the overall curvature (d) is decreasing, constant or increasing. This is done through the quadruple $[a, b, c, d]$ with $a, b, c, d \in \{-1, 0, +1\}$. (For a formal definition and an illustration, see [1].)

The categories of direct and indirect contact state transitions are separately investigated. In the first case, continuous slope changes that require a more accurate analysis of the complete signal curves are expected. In the second case discontinuities at the point of transition are predicted; thus, the analysis focuses on this specific point.

Here, one example from each of the above categories is examined in detail. As direct contact state transition, the E/E→E/F transition is chosen, since the analysis is clear while still demonstrating the method. The investigation of the indirect transitions is exemplified using the E/E→E/V→E/E transition. For a complete analysis please, see [11].

3. Example for direct transitions

The analysis of the E/E→E/F transition is presented here as one example of a direct transition. There are several ways to generate this transition. The robot motion direction can vary from perpendicular to parallel to the face F. Here, the motion direction is assumed to be perpendicular to the edge E and parallel to the face F, as illustrated in Figure 1. The gripper is at height t above the face F and inclined at angle β. The horizontal distance between the gripper and the edge E is z. During the transitional motion, z increases while t and β remain constant. The direction θ of the reaction force R thus increases to a maximum of 90° and remains constant after transition.

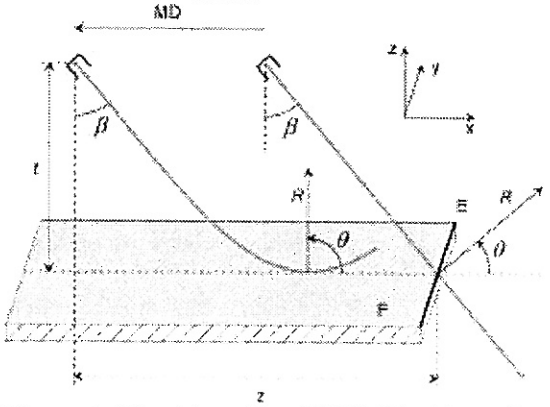

Figure 1: Direct transition E/E→E/F with motion direction MD perpendicular to E and parallel to F.

Interesting are the curves for the reaction components $R_{\perp}$, perpendicular to the face F, and $R_{//}$, perpendicular to the edge E and parallel to the face F. Both are regarded as a function of the distance z between the gripper and the edge E ($z \geq \tan(\beta) \cdot t$; for $z < \tan(\beta) \cdot t$ there is no contact).

We assume an initially straight, homogeneous, and lowly elastically deformable (deformation class E– in [3]) DLO. Thus, the shape of the DLO can be approximated by a cubic curve in the Cartesian coordinate system, with its origin in the gripper and the X-axis parallel to the undeformed DLO. Friction is neglected. Detailed analysis and explanations for the formulae can be found in [11]; only final results are presented here.

The point of contact between the DLO and the edge E / face F has the coordinates (t', z'), defined as:

$$t' = \cos(\beta)\cdot t + \sin(\beta)\cdot z$$
$$z' = \cos(\beta)\cdot z + \sin(\beta)\cdot t$$

The DLO shape $y(x)$ is then described by the equation C_1 in the pre-transition phase ($0 = z' = z'_0$) and by C_2 in the post-transition phase ($z'_0 = z'$). Both equations are obtained from a general cubic polynomial, in which all parameters can be expressed in terms of z', t' and β. As boundary conditions, the known position of the gripper and the DLO orientation forced by the gripper are used. For C_1, the fixed position of the point contact at the edge E is used additionally; for C_2, it is clear there must be a DLO tangent parallel to the face F. For both equations, the deformation energy is minimized while the overall curvature is kept positive. C_1 and C_2 are given as:

$$C_1 : y(x) = -\frac{z'}{2t'^3}x^3 + \frac{3z'}{2t'^2}x^2$$

$$C_2 : y(x) = -\frac{\cot(\beta)^3}{27(\cot(\beta)t'-z')^2}x^3 + \frac{\cot(\beta)^2}{3(\cot(\beta)t'-z')}x^2$$

The transition takes place at "time" z_0 or z'_0, when the DLO tangent at edge E is parallel to face F:

$$z'_0 = \frac{2t'\cot(\beta)}{3} \Leftrightarrow z_0 = \frac{(2+\sin(\beta)^2)t}{\cos(\beta)\sin(\beta)}$$

The bending moment is proportional to the second derivative of the shape: $M = M(0) = y''(0)EI$ with E describing the elasticity and I the inertia of the DLO. Thus, before transition the moment M is

$$M = \frac{3z'}{t'^2}EI = \frac{3\cos(\beta)z - 3\sin(\beta)t}{(\cos(\beta)t + \sin(\beta)z)^2}EI$$

and after transition it is

$$M = \frac{2\cot(\beta)^2}{3(\cot(\beta)t'-z')}EI = \frac{2\cos(\beta)^2}{3t\sin(\beta)}EI = const$$

Dividing the bending moment M by the length of the actual lever arm provides the actual force R. The components of interest are the coordinates ($R_{//}$, $R_\perp$) of R in the initial coordinate system. Before transition, the components

$$R_{//} = \frac{2t'\cos(\beta) - 3z'\sin(\beta)}{2t'^2+3z'^2}M$$
$$R_\perp = \frac{2t'\sin(\beta) + 3z'\cos(\beta)}{2t'^2+3z'^2}M$$

are observed; after transition, they are

$$R_{//} = 0$$
$$R_\perp = \frac{M}{(\cos(\beta)t'-\sin(\beta)z')(2\cot(\beta)+3\tan(\beta))}$$
$$= \frac{2\cos(\beta)^2}{3t^2\sin(\beta)(2\cot(\beta)+3\tan(\beta))}EI = const$$

Figure 2 shows the curves for the reaction components and the bending moment.

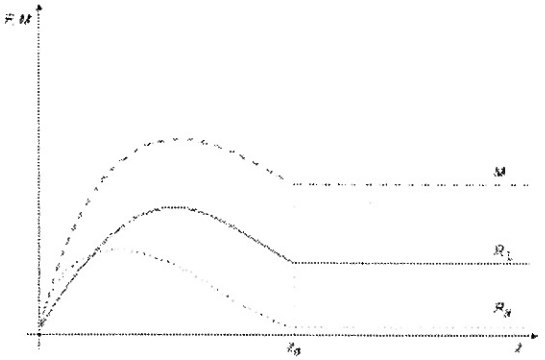

Figure 2: Expected curves of forces $R_{//}$, $R_\perp$ and moment M of a direct E/E→E/F transition, with motion direction perpendicular to E and parallel to F as a function of distance z between gripper and E.

For experimental verification, we take the situation from Figure 1. The Cartesian coordinate system for measurements has its Z-axis pointing upwards perpendicular to the face F, its Y-axis parallel to the edge E and its X-axis pointing to the right. As DLO, we use a 30 cm steel ruler. The gripper inclination β is 30° and the gripper is about $t = 6$ cm above the table with a horizontal distance of about $z = 5$ cm to the edge E. Thus, the angle between the face F and the DLO tangent at the contact point is about 57° implicating a slight initial tension of the DLO. Robot speed is 10 mm/s. Force measurements are taken every 100 ms. The low-pass filtered E/E→E/F transition signals are displayed in Figure 3.

For better comparison with the theoretical results, the sensor data is inverted in accordance to the role the components play: F_x corresponded to $R_{//}$, F_z to $R_\perp$ and $-M_y$ to M.

It should be pointed out that the initial tension was artificially set to zero at the start of robot motion. This explains why the increasing part of F_x is missing, and why the initial force measurements are higher than those after transition. Additionally, the discontinuities in F_x and F_z at the beginning of robot motion (measurement) are due to static friction. With this taken into account, the signals fulfill our theoretical expectations.

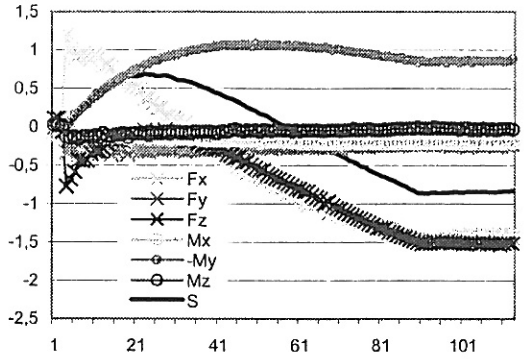

Figure 3: Forces F_x, F_y, F_z, moments M_x, M_y, M_z, and observation curve S of a direct E/E→E/F transition with motion direction perpendicular to E and parallel to F.

The transition occurs around measurement 90, and can easily be observed in the moment and in both force curves. For detection, the directions of the reaction force at the beginning of robot motion and of the resulting moment are chosen. The direction of the reaction force changes and the statically observed component suffers an additional decreasing effect. As both the moment and the initial reaction force component signals vary the same way, they are combined into one linear combination to be observed for detection. In the example situation, the observation direction is given as:

$$S = \frac{1}{\sqrt{2}}\left(\cos(57°)F_x + 0F_y + \sin(57°)F_z\right) + \frac{1}{\sqrt{2}}\left(0M_x - 1M_y + 0M_z\right)$$

The predicted curve is describable as piecewise linear function by: no discontinuity ($a = 0$), negative slope ($b = -1$), transition, constant slope ($c = 0$), increasing curvature ($d = +1$).

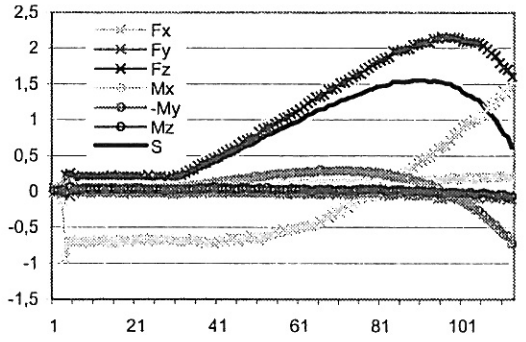

Figure 4: Forces F_x, F_y, F_z, moments M_x, M_y, M_z, and observation curve S of a direct E/F→E/E transition with motion direction parallel to F and perpendicular to E.

For the backwards transition E/F→E/E, an inverted behavior is predicted. However, the experimental results in Figure 4 do not exactly fit this prediction. In fact, all measurements are artificially set to zero at the start of robot motion, and there is a remaining tension after the robot motion stopped, explaining why the constant parts all have the same initial value, why decreasing part of F_x is missing and why the F_z component value ends higher than it starts.

The discontinuity in F_x at the beginning of robot motion is due to static friction and can be neglected. Additionally, the F_x ($R_{//}$) force signal seems shifted to the right. In fact, the sliding friction force is opposed to the reaction component F_x ($R_{//}$), with their growth-behavior inverted.

The transition is situated around measurement 30. It can easily be detected in both the moment M_y (M) and F_z ($R_\perp$) force curve. Still, the direction of the reaction force at the beginning of robot motion is chosen for detection. In the initial situation, it does not contain the F_x ($R_{//}$) component. As both the moment and the initial reaction force component signals vary in the same way, after linear combination, the transition is still detectable. In our example situation, the observation direction is:

$$S = \frac{1}{\sqrt{2}}\left(0F_x + 0F_y + 1F_z\right) + \frac{1}{\sqrt{2}}\left(0M_x - 1M_y + 0M_z\right)$$

The expected curve can be described as piecewise linear function by: no discontinuity ($a = 0$), constant slope ($b = 0$), transition, positive slope ($c = +1$), increasing curvature ($d = +1$).

4. Example for indirect transitions

As analysis of direct contact state transitions has been demonstrated, the next case is indirect transitions. The $E/E_1 \rightarrow E/V \rightarrow E/E_2$ transition is presented here as one example.

For this investigation, we use a DLO deformable only in the plane perpendicular to the first obstacle edge E_1. The gripper is moved with constant speed parallel to E_1 in the direction of E_2, and the angle between E_1 and E_2 is α. See Figure 5.

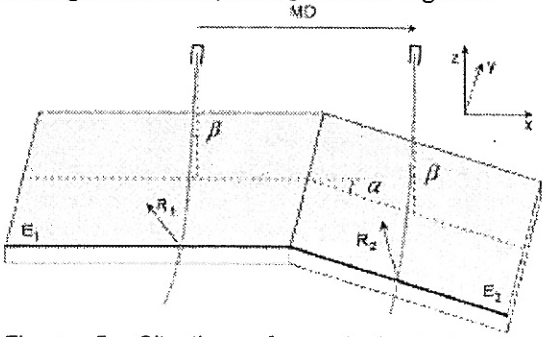

Figure 5: Situation of an indirect transition $E/E_1 \rightarrow E/V \rightarrow E/E_2$. The DLO is deformable within only one plane perpendicular to the Edge E_1.

Before transition, the reaction force R_1, perpendicular to E_1 and the DLO tangent at the contact point, is quite obvious. After transition, reaction force R_2 remains, perpendicular to E_2 and the DLO tangent at the contact point. The base directions $R_\perp$ and $R_{//}$ are defined, parallel to R_1 and parallel to E_1 in the direction of E_2, respectively. Thus, R_1 and R_2 can be expressed as components of $R_\perp$ and $R_{//}$. Force $R_\perp$ produces a moment $M_{//}$ around an axis parallel to E_1, and $R_{//}$ produces a moment $M_\perp$ around an axis perpendicular to E_1 and the DLO tangent at the contact point.

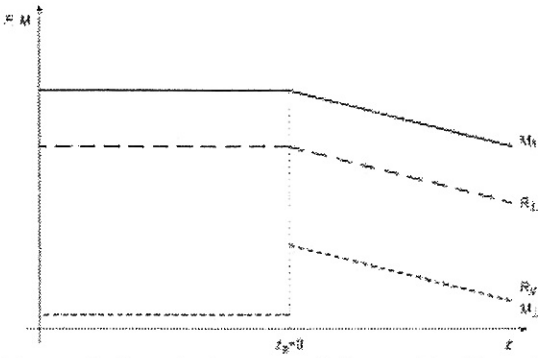

Figure 6: Expected curves of forces $R_{//}$, $R_\perp$ and moments $M_{//}$, $M_\perp$ of an indirect transition $E/E_1 \rightarrow E/V \rightarrow E/E_2$ as a function of the distance z between gripper and Edge E_2. The DLO was deformable in only one plane.

Before the transition, all force and moment components are constant and $R_{//}$ and $M_\perp$ are known to be zero. At the transition point, the DLO shape is assumed to remain constant (the DLO is only deformable in the plane perpendicular to the edge E_1). Thus, the initial bending moment $M_{//}$ remains constant, as does the initial force component $R_\perp$. The reaction force R_2 has a non-zero $R_{//}$ component because the $R_\perp$ component is equal to R_1, resulting in a non-zero $M_\perp$ moment component. After the transition, all force and moment components decrease with decreasing deformation of the DLO. The expected signal curves are shown in Figure 6 and can be described as follows: no discontinuity ($a = 0$) or positive discontinuity ($a = +1$), constant slope ($b = 0$), transition, negative slope ($c = -1$), decreasing curvature ($d = -1$).

For the experimental verification shown in Figure 7, we take the situation from Figure 5. The Cartesian coordinate system used has its X-axis parallel to edge E_1 in the direction of E_2 and its Y-axis in the plane of the outlined face. The angle α between the edges E_1 and E_2 is 45°. The gripper is about 6 cm above the table with a horizontal distance of about 12 cm to the edge E_1. All other parameters are as in Section 3. Thus, the angle between the face F and the DLO tangent at the contact point is about 15°. For better comparison with the theoretical results, the sensor data is inverted according to the role the components play: F_x corresponds to $R_{//}$, $-F_y$ and F_z to $R_\perp$, $-M_x$ to $M_{//}$, and finally, $-M_y$ and M_z correspond to $M_\perp$.

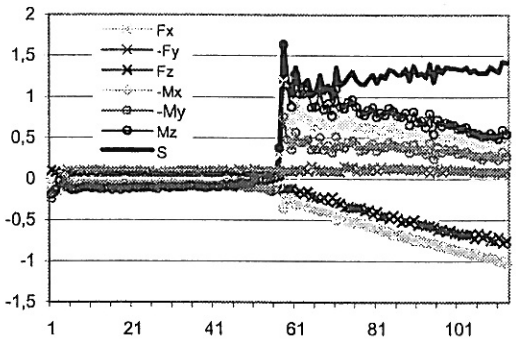

Figure 7: Forces F_x, F_y, F_z, moments M_x, M_y, M_z, and observation curve S of an indirect $E/E_1 \rightarrow E/V \rightarrow E/E_2$ transition. The DLO was deformable in the Y-Z-plane

Again, the measurement components are all artificially set to zero at the start of robot motion, which explains why the constant portions all start with the same value.

At first sight, the signals are as predicted. Upon more detailed viewing, a slight discontinuity in the moment component $-M_x$ ($M_{//}$) and in the force component F_z ($R_\perp$) is visible, although these components are expected to be continuous. In fact, at transition, the steel ruler used as DLO is slightly deformed out of the main deformation plane. As the overall bending is not increased, it cannot be expected that the value of the initial moment component is maintained when the axis is moved. The initial force component changed accordingly.

The transition is situated around measurement 58 and can easily be detected by looking for discontinuities. Changing the assumption about DLO deformation at transition, the explanation above is used to make transition detection using discontinuities more robust by taking advantage of the increasing effect of subtracting a negative from a positive discontinuity.

For detection, both the difference between the initial force direction $R_\perp$ and the resulting force direction $R_{//}$ and that between the initial moment axis $M_{//}$ and the resulting moment direction $M_\perp$ have to be observed. Both differences exhibit the same discontinuities. Unfortunately, neither the slope nor the overall curvature can be determined after transition. In our sample situation the observation direction is given as:

$$S = \frac{1}{\sqrt{2}}\left(F_x - \left(-\sin(15°)F_y + \cos(15°)F_z\right)\right)$$
$$+ \frac{1}{\sqrt{2}}\left(\frac{1}{\sqrt{2}}\left(-M_y + M_z\right) - \left(-M_x\right)\right)$$

The expected signal curve can be described piecewise linear function by: positive discontinuity ($a = +1$), constant slope ($b = 0$), transition, unknown slope ($c = ?$), unknown curvature ($d = ?$).

5. Complete list of characteristics

Using the same method as described in Section 2 and illustrated in Sections 3 and 4, a significant observation direction together with a piecewise linear function approximating the characteristic signal curve is determined for each of the 21 contact state transitions plus variants. To completely list the observation directions, the following is defined:

- R_F as reaction force direction of face F, perpendicular to this face F,
- R_E as reaction force direction of edge E, perpendicular to edge E and the DLO tangent at the contact point,
- $R_{X,0}$ as starting reaction force direction
- $R_{X,T}$ as expected reaction force direction after transition
- $R_{X,\perp}$ as reaction force component appearing at transition and perpendicular to R_X
- M_X as moment axis of the reaction force F_X
- $M_{X,0}$ as starting moment axis
- $M_{X,T}$ as expected moment axis after transition
- $M_{X,\perp}$ as moment axis of the reaction force $R_{X,\perp}$

These general directions can be obtained automatically from transition-specific geometric data, either provided by a robot simulation system or by the user. For a specific transition situation, the directions are calculated as a linear combination of the sensor's six measurement dimensions. The complete list of transition characteristics is given in table 1.

To handle more than one contact at a time, e.g. establishing contact while maintaining the actual contact situation unchanged, required to achieve complex assemblies, it may become necessary to observe only the force and moment opposed to the motion direction.

6. Conclusions

All contact state transitions are implemented using Adept's V+ robot language on a Stäubli RX130 with a 90M31A force/torque sensor from JR3.

In a first version, a primitive algorithm is used to search for the predicted characteristics in the sensor data. At each step, a window consisting of the last $N + M$ measuring points is considered. The linear regression D over the first N measurements as well as the standard error σ is calculated. If more than R% of the next M measurements have a distance to D greater than σ, and if those measurements diverge in the right direction, it is assumed that the transition has taken place. Of course, the linear regression is checked for the expected slope before enabling the evaluation of the final detection condition. Other detection algorithms can be found in [10] and [12].

Transition	Observation		Signal
	Force	Moment	
N→V/F	$R_{F,T}$	$M_{F,T}$	(0,0,1,1)
N→E/F	$R_{F,T}$	$M_{F,T}$	(0,0,1,1)
N→E/E	$R_{E,T}$	$M_{E,T}$	(0,0,1,1)
V/F→N	$R_{F,0}$	$M_{F,0}$	(0,-1,0,1)
E/F→N	$R_{F,0}$	$M_{F,0}$	(0,-1,0,1)
E/E→N	$R_{E,0}$	$M_{E,0}$	(0,-1,0,1)
V/F→V/E→N	$R_{F,0}$	$M_{F,0}$	(-1,0,?,?)
E/F→E/V→N	$R_{F,0}$	$M_{F,0}$	(-1,0,?,?)
E/E→E/V→N	$R_{E,0}$	$M_{E,0}$	(-1,0,?,?)
E/E→V/E→N	$R_{E,0}$	$M_{E,0}$	(-1,?,?,?)
V/F→E/F	$R_{F,0}$	$M_{F,0}$	(0,1,1,1)
E/F→V/F	$R_{F,0}$	$M_{F,0}$	(0,-1,-1,1)
E/E→E/F[1]	$R_{E,0}$	$M_{E,0}$	(0,-1,0,1)
E/F→E/E[1]	$R_{F,0}$	$M_{F,0}$	(0,0,1,1)
E/E→E/F[2]	$R_{F,T}$	$M_{F,T}$	(0,1,1,1)
E/F→E/E[2]	$R_{F,0}$	$M_{F,0}$	(0,-1,-1,1)
E/E_1→E/V→E/E_2	$R_{E1,\perp}$ $-R_{E1}$	$M_{E1,\perp}$ $-M_{E1}$	(1,0,?,?)
E/E→E/V→E/F	$R_{E,\perp}$ $-R_E$	$M_{E,\perp}-M_E$	(1,0,?,?)
E/F_1→E/V→E/F_2	$R_{F1,\perp}$ $-R_{F1}$	$M_{F1,\perp}$ $-M_{F1}$	(1,0,?,?)
E/F→E/V→E/E	$R_{F,\perp}$ $-R_F$	$M_{F,\perp}-M_F$	(1,0,?,?)
V/F_1→V/E→V/F_2[3]	$R_{F1,\perp}$ $-R_{F1}$	$M_{F1,\perp}$ $-M_{F1}$	(1,0,?,?)
V/F_1→V/E→V/F_2[4]	R_{F1} $-R_{F1,\perp}$	$M_{F1,0}$	(-1,0,-1,-1)
V/F_1→V/E→V/F_2[5]	R_{F1} $+ R_{F1,\perp}$	$M_{F1,0}$	(1,0,-1,-1)
E/E→V/E→V/F	$R_{F,\perp}-$ R_F	None	(-1,?,0,?)
V/F→V/E→E/E	$R_{F,\perp}-$ R_F	None	(1,0,?,?)

1: motion direction parallel to F
2: motion direction perpendicular to F
3: DLO perpendicular to motion direction
4: DLO pointed in motion direction
5: DLO pointed opposed to motion direction

Table 1: Transition characteristics

The robustness of detection is tested for several examples. As a DLO we use a polyamide hose (20 cm long, 6 mm outer and 4 mm inner diameter). Stainless steel obstacles were designed to

combine many (even complex) contact state transitions. See Figure 8. To reduce friction, a steel ball of 6 mm diameter is fitted to the end of the DLO.

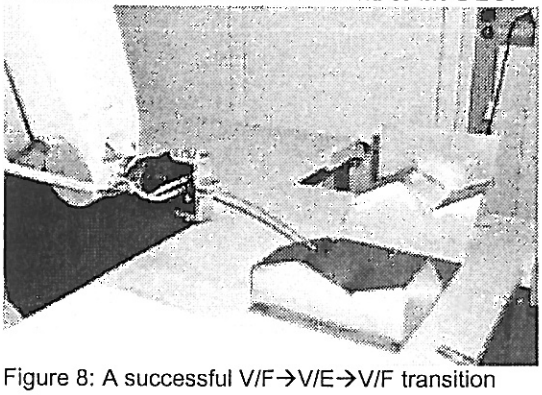

Figure 8: A successful V/F→V/E→V/F transition

Transitions characterized by a constant slope before transition can reliably be detected by our primitive detection algorithm. Series of experiments show that reliability of detection is better than 95% with no observable friction, whereas it rapidly drops below 50% with increasing effects of static friction during movement. (DLO sticks to the obstacle, bends, snaps forwards, ...) Most of the practice-relevant transitions (like establishing contact, indirect loss of contact or indirect contact change) belong to this category.

The direct loss of contact, the transition E/F→E/E with motion direction perpendicular to F, the E/F→V/F transition, and the E/E→E/F transitions are not correctly detected by the algorithm, as the expected force signals before transition are not really linear. However, we believe that most of these transitions can be detected by a more sophisticated detection algorithm.

Nevertheless, as all possible contact state transitions are available in a library of V+ macros, programming some DLO manipulation tasks is becoming easier. The programmer no longer needs do cope with a huge amount of raw sensor data. This is all transparently done by the library. Robot programs for assembly tasks may to a certain degree even be generated automatically from some of the task's geometric data and its contact state transition map using those manipulation skills.

References

[1] Abegg F., Remde A., and Henrich D.: "Force- and vision-based detection of contact state transitions". In: Robot manipulation of deformable objects, Henrich D., Wörn H. (Eds.), Springer-Verlag, London, 2000, ISBN: 1-85233-250-6, pp. 111-134

[2] Hasegawa T., Suehiro T., and Takase K.: "A model-based manipulation system with skill-based execution". In: IEEE Transactions on Robotics and Automation, vol. 8, No. 5, pp. 535-544, October 1992.

[3] Henrich D., Ogasawara T., Wörn H.: "Manipulating deformable linear objects: Contact states and point contacts". In: Proc. 1999 IEEE International Symposium on Assembly and Task Planning (ISATP'99), Porto, Portugal, July 21-24, 1999.

[4] Kraus W., McCarragher B. J.: "Case studies in the manipulation of flexible parts using a hybrid position/force approach". In: Proc. 1997 Int. Conf. on Robotics and Automation (ICRA'97), vol. 1, pp. 367372, Albuquerque, USA, April, 1997.

[5] Morris G. H., Haynes L. S.: "Robotic assembly by constraints". In: Proc. 1987 IEEE Int. Conf. on Robotics and Automation (ICRA'87), pp. 1507-1515.

[6] Morrow J. D., Khosla P. K.: "Manipulation task primitives for composing robot skills". In: Proc. 1997 IEEE Int. Conf. on Robotics and Automation (ICRA'97), pp. 3354-3359, Albuquerque, USA, April 1997.

[7] Morrow J. D., Nelson B. J., Khosla P. K.: "Vision and force driven sensorimotor primitives for robotic assembly skills". In: Proc. 1995 IEEE/RSJ Int. Conf. on Intelligent Robots and Systems (IROS'95), Pittsburgh, Pennsylvania, USA, August 1995.

[8] Nakagaki H., et al.: "Study of deformation and insertion tasks of a flexible wire". In: Proc. 1997 Int. Conf. on Robotics and Automation (ICRA'97), vol. 3, pp. 2397-2402, Albuquerque, USA, April 1997.

[9] Remde A., Henrich D., and Wörn H.: "Manipulating deformable linear objects: Contact state transitions and transition conditions". In: 1999 IEEE/RSJ Int. Conf. on Intelligent Robots and Systems (IROS'99), Kyongju, Korea, October 1999.

[10] Remde A., Pfaffenberger E., and Wörn H.: "Manipulating deformable linear objects: Force based detection of contact state transitions". In: 2000 IEEE/RSJ Int. Conf. on Intelligent Robots and Systems (IROS'2000), Takamatsu, Japan, October/November 2000.

[11] Schlechter A.: "Manipulation of deformable linear objects: Analysis and implementation of macro operations", Diploma Thesis (in German), Faculty of Informatics, University of Kaiserslautern, Germany, September 2000.

[12] Torres E.: "Manipulation of deformable linear objects: Detection of contact state transitions", Diploma Thesis (in German), Faculty of Informatics, University of Kaiserslautern, Germany, March 2001.